

## Tuning interchain and intrachain interactions in polyfluorene copolymers

Ya-Shih Huang,<sup>1,\*</sup> Johannes Gierschner,<sup>2</sup> Johanna P. Schmidtke,<sup>1</sup> Richard H. Friend,<sup>1</sup> and David Beljonne<sup>3,\*</sup>

<sup>1</sup>*Cavendish Laboratory, JJ Thomson Avenue, Cambridge, CB3 0HE, United Kingdom*

<sup>2</sup>*Madrid Institute of Advanced Studies—IMDEA in Nanoscience, Facultad de Ciencias Módulo C-IX, 3ª planta, Avda. Tomás y Valiente, 7, Ciudad Universitaria de Cantoblanco, 28049, Madrid, Spain*

<sup>3</sup>*Laboratory for Chemistry of Novel Materials, University of Mons, Place du Parc 20, B-7000 Mons, Belgium*

(Received 27 July 2011; revised manuscript received 4 October 2011; published 14 November 2011)

We study how intermolecular interactions, conformational changes, and polarization effects control the nature of the electronic excitations in conjugated polymer blends. Quantum-chemical calculations and high-pressure photoluminescence experiments are used to assess these effects in polyfluorene-based donor–acceptor systems. The redshift of charge-transfer–like excitations usually observed under pressure is found to arise primarily from the reduced interchain distance; the corresponding shift of bulk excitons is equally sensitive to the interchain spacing and planarization alterations. Intermolecular charge-transfer states are shown to have shorter radiative lifetimes and higher oscillator strengths at high pressure. In contrast, intramolecular bulk excitons build up interchain charge-transfer character and lose oscillator strength and radiative efficiency with increasing pressure.

DOI: [10.1103/PhysRevB.84.205311](https://doi.org/10.1103/PhysRevB.84.205311)

PACS number(s): 62.50.–p, 71.20.Rv, 73.20.–r, 78.55.–m

### I. INTRODUCTION

Conjugated polymers have been widely investigated for their advantages of flexibility and ease of solution processing, which make them promising candidates for both large-area and low-cost optoelectronic applications.<sup>1–4</sup> Their electronic and photophysical characteristics are closely related to the chemical structure of the monomer units and the conformational space the polymer chains can explore, as well as their packing in the solid. In contrast to the limiting situation of isolated single chains supporting only intrachain excitations,<sup>5–7</sup> interchain interactions impact the electronic and optical properties of multichromophoric systems and subsequently govern the operation of optoelectronic devices based on organic semiconductors.<sup>8–10</sup> Organic light-emitting diodes and photovoltaic cells typically consist of an electron donor component and an electron acceptor component for the purpose of tuning optical and electrical properties, and their interfaces play an important role in the device performance. We previously established a model, showing that a variety of interchain excitations form at the polymeric heterojunction, depending on the precise interfacial alignment of polymer chains, and are accompanied by the occurrence of intrachain bulk excitons.<sup>11</sup>

There have been several approaches developed to probe intramolecular versus intermolecular interactions. Applying hydrostatic pressure has been demonstrated as a clean method to vary interchain interactions and to change molecular conformations of several conjugated polymers without chemical modifications.<sup>12–18</sup> Work by Schmidtke *et al.* on polyfluorene donor–acceptor (D-A) systems in solid-state solution and film has ascribed the photoluminescence (PL) redshift under hydrostatic pressure in the solid-state solution to planarization of the polymer backbones, and the additional PL redshift observed in films was attributed to interchain interactions and refractive index change under pressure.<sup>16,17</sup> A recently published report on pressure studies of similar systems probed not only the emissive but also the nonemissive excited states and highlighted the important impact of changes in the dielectric medium under pressure.<sup>18</sup> More specifically, the applied pressure was found to yield an increased dielectric

constant, which resulted in an enhanced charge-transfer (CT) character of the excitons.<sup>19</sup> Although we can likely trace the observed pressure effects to reduction of interchain separation, planarization of the polymer chains, and increase in density and dielectric constant, these contributions have not been systematically investigated thus far.

Such disentanglement might be not only important to elucidate the pressure experiments but also crucial to characterize the solid-state optical spectra of conjugated compounds. To study pressure effects at a theoretical level, density functional theory (DFT) has been implemented to study the band structure, dielectric tensors, and optical properties of some molecular crystals at varying intermolecular distances, which led to a qualitative picture of the pressure-induced bathochromic shifts.<sup>20</sup> Thin film polymers are, however, disordered systems with rather weak coupling between the chains, such that a model relying on the use of individual conjugated segments as building blocks for the bulk material might be more appropriate. Atomistic quantum-chemical methods have proved a powerful tool for the understanding of intrachain and interchain contributions to the solid-state electronic and optical properties, particularly by assessing the magnitude of excitonic/electronic couplings<sup>21,22</sup> and the influence of dimensionality,<sup>23</sup> as well as the intermolecular CT character in the lowest excited states<sup>24</sup> and the resulting impact on PL bandshapes.<sup>25</sup>

Thus, we establish here a theoretical treatment for the excited states in a polyfluorene D-A system as a function of the two primary parameters affected at high pressure, i.e., the intermolecular distance and the intramolecular torsion angle. In addition, we estimate the magnitude of the polarizability effect that can lead to an additional bathochromic shift by means of classical reaction field theory. The model systems investigated here are blends with the poly(9,9'-dioctylfluorene-*alt*-bis-*N,N'*-(4-butylphenyl)-bis-*N,N'*-phenyl-1,4-phenylenediamine) (PFB) poly(9,9'-dioctylfluorene-*alt*-*N*-(4-butylphenyl)diphenylamine) (TFB) as the donor and poly(9,9'-dioctylfluorene-*alt*-benzothiadiazole) (F8BT) as the acceptor [Fig. 1(a)].

The 1:1 blend of PFB:F8BT under pressure was recently investigated experimentally, which allows for a comparison with our calculations.<sup>17</sup> While the steady-state PL spectrum at ambient pressure is vibronically resolved with a maximum at 2.3 eV, the spectrum at 70 kbar is redshifted by 0.4 eV and lacks well-defined vibronic features.

## II. THEORETICAL METHODS

Single PFB, TFB, and F8BT chains with two, two, and five repeat units, respectively, were first optimized at B3LYP DFT level using the 6-31 basis set.<sup>26,27</sup> Their alkyl side chains were omitted to reduce computational time without significantly affecting the electronic excited-state properties.<sup>28</sup> PFB (or TFB) and F8BT chains were arranged in cofacial arrangements as model systems for PFB (or TFB):F8BT blends. Intermolecular arrangements with varying relative positions of the two molecules were optimized using the polymer consistent force field (PCFF) based on a 9-6 Lennard-Jones potential<sup>29</sup> with the conjugated backbones frozen to the DFT results. Such optimizations only adjust intermolecular parameters while keeping intramolecular constraints such as torsion angles fixed. The optimized intermolecular distance between PFB/TFB and F8BT was found to be  $\sim 4.5$  Å, and the torsion angles between poly(9,9'-dioctylfluorene) (F8) and benzothiadiazole (BT) in the F8BT chain were  $\sim 35^\circ$ . Based on these ground-state geometries, a semiempirical Zerner's intermediate neglect of differential overlap (INDO)<sup>30</sup> with a screened Mataga-Nishimoto potential<sup>31,32</sup> was coupled with single configuration interaction (SCI) scheme to characterize the excited-state properties of the two-chain system in terms of transition energies, charge redistributions, oscillator strengths, and transition dipole moments.

To assess in an approximated way, the spectral shift associated with the increased polarizability upon increasing pressure was studied using the Onsager equation, which relates the spectral shift  $\Delta E_{\text{abs/pl}}$  to the refractive index  $n$  of the environment<sup>33</sup>:

$$\Delta E_{\text{abs/pl}} = A \cdot (n^2 - 1)/(2n^2 + 1), \quad (1)$$

where the slope  $A$  contains information about cavity size, oscillator strength, and energy of the transition considered. The density  $\rho$  dependence of the refractive index can be obtained via the molar refraction, which should be constant for a given material:

$$R = (M/\rho) \cdot (n^2 - 1)/(n^2 + 2) = V_m \cdot (n^2 - 1)/(n^2 + 2), \quad (2)$$

where  $M$  is the molar weight and  $V_m$  is the molar volume.  $R$  can be expressed by the atomic refractions,  $R = \sum N_i \cdot R_i$ , where  $N_i$  is the number of each atom;  $R_i$  values for the atoms in F8BT were taken from literature.<sup>34</sup>

Earlier INDO/SCI calculations came to the conclusion that, depending on the mutual orientation of the copolymer repetition units, PFB/TFB:F8BT blends support *interchain* CT excitons and *intrachain* F8BT bulk excitons as the lowest electronic excitations.<sup>11</sup> Figure 1(b) summarizes the electronic properties of these excited states. CT excitons include polaron pairs and exciplexes, in which the excited electrons are on the BT unit of F8BT and holes are on the triarylamine of

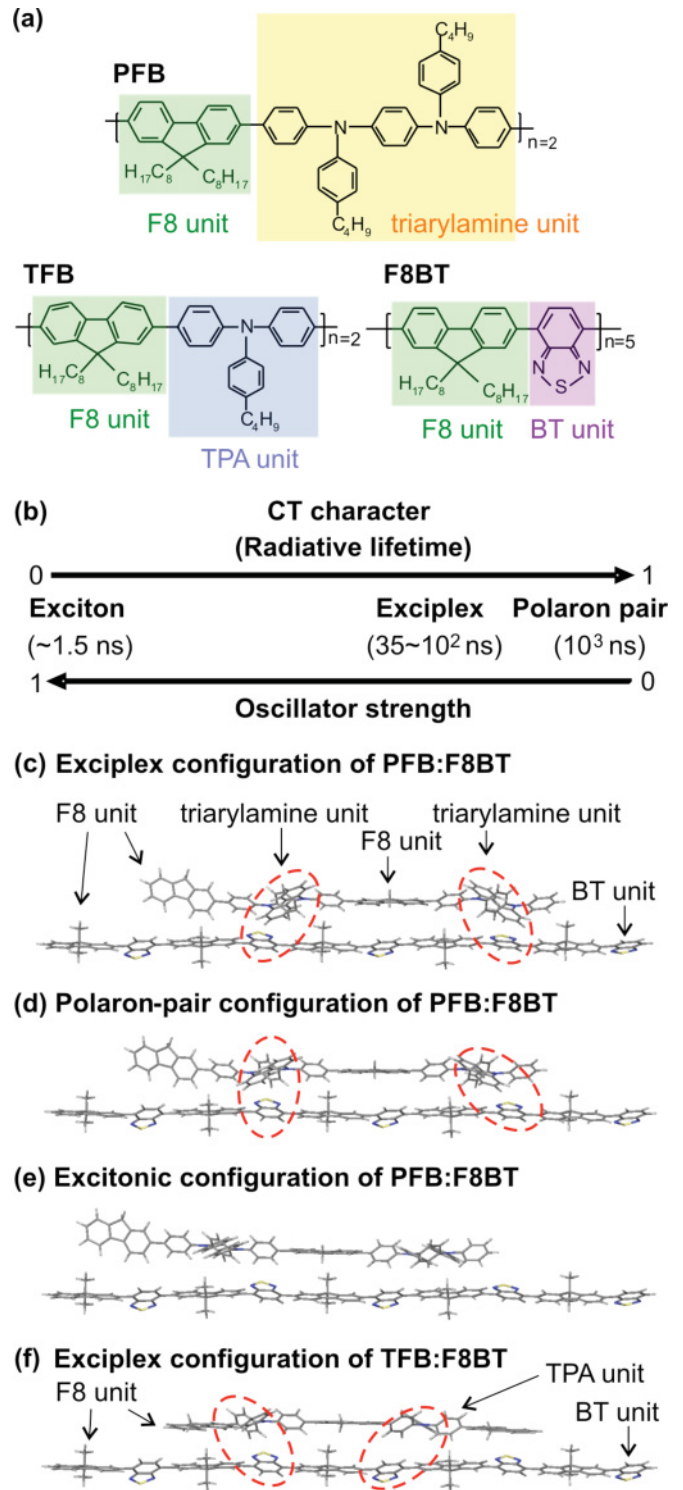


FIG. 1. (Color online) (a) Chemical structures of model compounds. (b) Illustration of the excited-state characteristics formed at D-A heterojunctions. Representative DFT and PCFF-optimized ground-state structures supporting (c) exciplexes, (d) polaron pairs, and (e) excitons in PFB:F8BT and (f) exciplexes in TFB:F8BT. The investigated systems contain two and five repeat units of PFB/TFB and F8BT, respectively. Dashed (red) circles indicate where the primary interaction occurs.

PFB/TFB. While exciplexes are a hybrid excited state with strong CT character ( $>90\%$ ) mixed with a small fraction

of local excitation, polaron pairs are nearly ionic ( $\sim 99\%$ ). Furthermore, PFB:F8BT polaron pairs are found to have lifetimes of thousands of nanoseconds as a result of very small oscillator strengths associated with the strong CT character and may recombine into F8BT triplet excitons within 40 ns.<sup>35</sup> On the other hand, exciplexes show lifetimes of tens to hundreds of nanoseconds with redshifted emissions. The transition dipole moments of CT states have considerable contributions from the stacking direction that is perpendicular to the excitonic (along the chain) axis. Unlike these CT states, F8BT excitons are formed as a result of intrachain interactions and show both short radiative lifetimes and high oscillator strengths.

We selected several DFT/PCFF-optimized ground-state geometries that yield these species as the lowest excited states for the investigations of the interchain separation and planarization effects [Fig. 1(c)–1(f)]. The ground-state geometries where the triarylamine units of PFB are right and nearly on top of the BT units of F8BT lead to polaron pairs and exciplexes, respectively, as the lowest excited state; the geometries with the F8 units of PFB on top of the BT units of F8BT instead stabilize F8BT excitons. Although there are only slight differences between the ground-state geometries that give rise to polaron pairs and exciplexes, the impact on the radiative lifetime, as well as oscillator strength, is significant. The oscillator strength of the polaron pairs is found to be at least one order of magnitude smaller than that of the exciplexes.

To assess the influence of planarization, we reduced the torsion angles between F8 and adjacent BT units of the F8BT chain for different D-A arrangements, from  $35^\circ$ , to  $30^\circ$ ,  $27^\circ$ , and  $25^\circ$ . Minimization of the intermolecular geometric parameters at the DFT/PCFF level yields an equilibrium interchain separation of  $\sim 0.45$  nm. For the study of the intermolecular separation dependence, the distance between the chains was decreased in the range 0.01–0.05 nm. X-ray diffraction studies of polythiophenes have shown a 5%–15% reduction in intermolecular distance at pressures of 80 kbar;<sup>36</sup> modeling with a  $(0.5/4.5) = 0.11 = 11\%$  reduction in the stacking separation thus appears to be reasonable for this study. The resulting ground-state geometries with varying orientations, interchain distance, and torsion angles were then used as input for INDO/SCI excited-state calculations. The resulting excitation energies and corresponding transition dipole moments were converted into radiative lifetimes using the Einstein coefficient for spontaneous emission, in which the radiative lifetime  $\tau_{\text{rad}}$  for an emitter in vacuum with negligible reorganization energy can be expressed as

$$\tau_{\text{rad}} = \frac{3hc^3}{64\pi^4\nu^3\mu^2},$$

where  $\nu$  denotes the frequency of the electronic excitation and  $\mu$  is the corresponding transition dipole moment.

High-pressure experimental setup has been described elsewhere.<sup>17</sup>

### III. RESULTS AND DISCUSSIONS

#### A. Molecular orbital picture

In Fig. 2, we present the calculated energies of frontier molecular orbitals of PFB:F8BT from three energy levels lower than the highest occupied molecular orbital (HOMO)

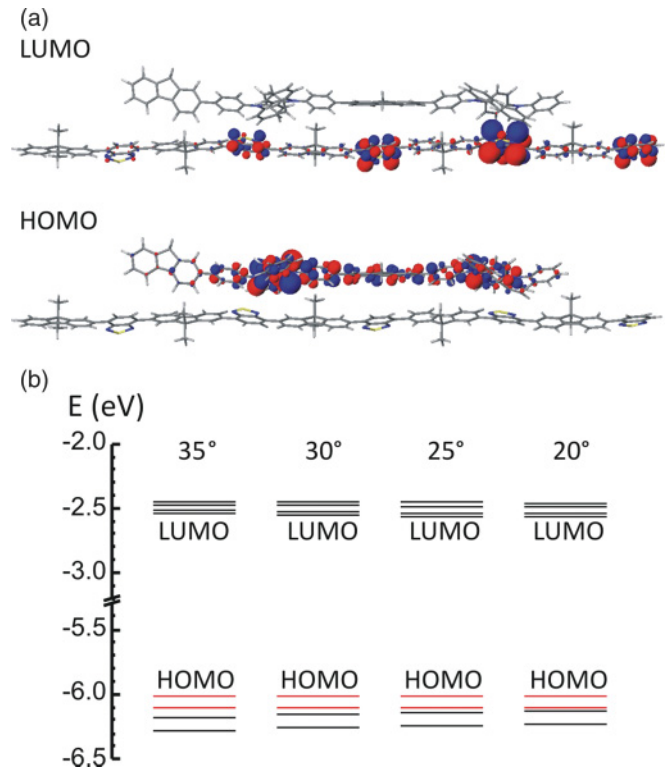


FIG. 2. (Color online) (a) Illustration of HOMO and LUMO topologies of F8BT. The size and color of each circle describe the amplitude and sign, respectively, of the linear combination of atomic orbitals coefficients associated with the  $\pi$  atomic orbitals. (b) Calculated frontier orbital energies of PFB:F8BT for a range of torsion angles. Black and red lines refer to molecular orbitals that are mostly confined on F8BT and PFB, respectively.

to three energy levels higher than the lowest unoccupied orbital (LUMO) for a range of torsion angles. The major consequence of planarization is observed in the shifting of the HOMO–2 level, while the other levels do not change significantly. This is expected, since the HOMO–2 orbital in the physical dimers corresponds to the HOMO of the F8BT chain, whose conformation is changed by tweaking the F8BT torsion angles (while, e.g., the HOMO and HOMO–1 orbitals are localized on the PFB segment). It has been established that the overall transition dipole moment of the lowest excited state in the complex can be approximated by the first-order perturbation theory, neglecting ground-state interactions, and higher-lying donor excited states as

$$\langle S_0 | \mu | XP \rangle \approx C_{\text{CT}} \langle H_{\text{PFB}} | \mu | L_{\text{F8BT}} \rangle + \frac{\langle H_{\text{PFB}} | h | H_{\text{F8BT}} \rangle}{E_{\text{EX}} - E_{\text{CT}}} \times \langle H_{\text{F8BT}} | \mu | L_{\text{F8BT}} \rangle, \quad (3)$$

where  $E_{\text{EX}}$  and  $E_{\text{CT}}$  denote the energies of pure local and CT electronic configurations, respectively;  $\langle H_{\text{F8BT}} | \mu | L_{\text{F8BT}} \rangle$  is the transition dipole moment of F8BT;  $\langle H_{\text{PFB}} | h | H_{\text{F8BT}} \rangle$  is the (one-electron) matrix element mixing of HOMOs of PFB and F8BT; and  $C_{\text{CT}} \approx 1$ . The resultant adiabatic states depend on the tradeoff of the transfer matrix element  $\langle H_{\text{PFB}} | h | H_{\text{F8BT}} \rangle$  and the energy mismatch  $\Delta E$  between pure local and CT electronic excitations. The rising HOMO–2 orbital confined on the F8BT chain with increasing planarization results in a

smaller energy mismatch  $\Delta E = E_{EX} - E_{CT}$  between local and CT configurations and thus brings about an increased excitonic character in the lowest CT-like excited state.

### B. Transition energies

Figure 3(b) shows the interchain distance and torsion angle dependence of calculated transition energies in PFB:F8BT. A remarkable decline in the computed transition energies is always observed with decreasing interchain distances in all geometric configurations. Our results agree quantitatively with the PL redshift probed in the high-pressure experiments [Fig. 3(a)], albeit the calculations were based on ground-state geometries. Moreover, the theoretical results suggest that the excitation energies calculated for ground-state structures that give rise to CT-like excited states are susceptible to the variation of interchain distance but not to planarization. This is correlated with the energy of such excited species being primarily controlled by interchain interactions. On the other

hand, the excitation energy of the covalent excitons is sensitive to the alteration of both the intermolecular distance and the torsion angle. High-pressure PL experiments have revealed that the redshift of exciplexes ( $370 \pm 50$  meV over 0.1 MPa to 9.1 GPa for PFB:F8BT blends)<sup>17</sup> is smaller than that of F8BT bulk excitons (530 meV over 0.1 MPa to 8.5 GPa),<sup>16</sup> even though the intermolecular compressibility was found to be greater than the intramolecular one.<sup>36</sup> Our results are able to shed some light on this. While reducing the interchain distance results in a similar decrease in transition energies for the excitonic and CT-like excitations, planarization reduces the energy of excitons more substantially than it does to CT states. As a combined effect of reducing interchain separation and planarization, the pressure application is thus expected to result in a larger reduction of the excitation energy for excitonic states than for CT states.<sup>17</sup>

The shift of  $\sim 0.15$ – $0.20$  eV calculated for exciplexes by accounting solely for the conformational and packing effects is underestimated compared to the PL data ( $\sim 0.4$  eV).<sup>16,17</sup> The difference is partly due to compressibility of the thin films and associated change in dielectric shielding. In this respect, the 0.05-nm reduction in the stacking distance would mean an anisotropic 11% reduction in volume, which is somewhat lower than the 20% at 75 kbar estimated in the pressure study of F8BT.<sup>18</sup> We can estimate the polarizability effect by considering the known compressibility of poly(octylthiophene) (which carries alkyl chains like in F8BT), where a volume reduction by 20% is found when going from 1 bar to 50 kbar, and the density at ambient pressure is 1.1 g/ml.<sup>36</sup> The slope  $A$  of the Onsager relation in Eq. (1) amounts to  $\sim 1$  eV, valid for a range of oligothiophenes.<sup>37</sup> Inserting all values in Eq. (1), the spectral shift induced by dielectric screening is estimated to be 0.05 eV going from 1 bar to 50 kbar. This is an isotropic model and thus does not account for specific excitonic interactions. Furthermore, when bringing two chains in a  $\pi$ -stacked arrangement closer, the specific excimeric/exciple effects give rise to additional low-frequency intermolecular vibronic coupling associated with larger CT character.<sup>24</sup> This may introduce large Huang-Rhys factors and an additional PL redshift (that can be as large as 0.2 eV) together with the loss of vibronic structure, as shown previously for a  $\pi$ -stacked molecular nanocrystals<sup>24</sup> and for a modeled dimer.<sup>25</sup>

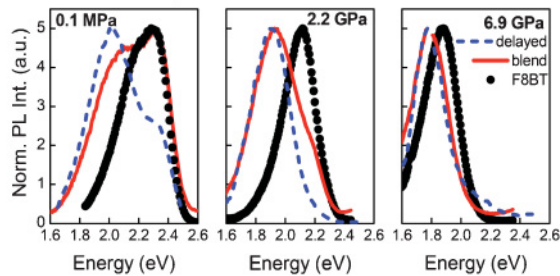
### C. Radiative lifetimes

Figure 3(c) presents calculated radiative lifetimes from the lowest excited states for a range of intermolecular distances and torsion angles in various PFB:F8BT ground-state geometries. For structures supporting polaron-pair states as the lowest excitations, the radiative lifetimes decrease with reducing interchain separation and increase with increasing planarization. When reducing the intermolecular distance by only 0.03 nm, the radiative lifetimes of polaron pairs drop to 1/2 or even to 1/3, reducing from a few thousands (characteristics of polaron pairs) to tens of nanoseconds (characteristics of exciplexes), due to the increase in oscillator strength.

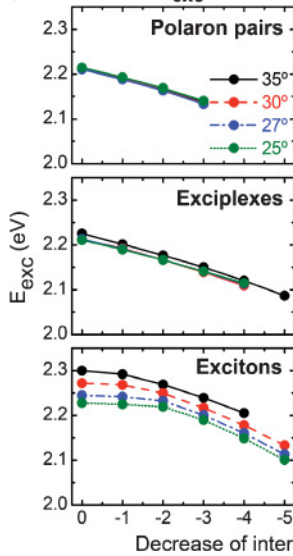
As for PFB:F8BT exciplex excitations, calculated radiative lifetimes  $\tau_{rad}$  are shortened upon decreasing *both* the interchain distance and the torsion angles in the ground-state geometries, which is consistent with the trend observed from the PL

## PFB:F8BT

### (a) Measured PL spectra



### (b) Calculated $E_{exc}$



### (c) Calculated $\tau_{rad}$

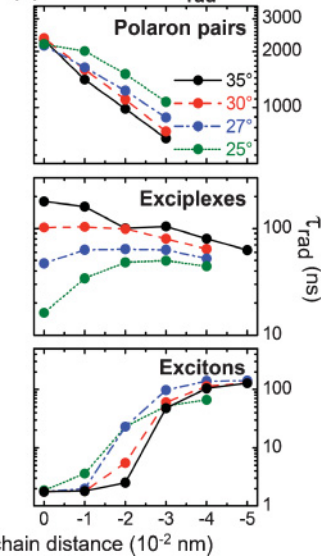


FIG. 3. (Color online) (a) Steady-state PL spectra (solid lines) of 1:1 PFB:F8BT-blended thin films at the indicated pressures. For comparison, steady-state spectra of a F8BT thin film (symbols) are shown for the same pressures. The delayed emission spectra (dashed line) of the blends were integrated 50–100 ns after excitation. (b) INDO/SCI excitation energies and (c) calculated radiative lifetimes of the lowest excited states for representative polaron-pair, exciplex, and excitonic geometries in PFB:F8BT blends as a function of interchain distance and torsion angle.

lifetimes  $\tau$  measured in high-pressure experiments<sup>17,38</sup> [Fig. 4(a)]. The experimental decay rates  $k = 1/\tau$  are the sum of radiative and nonradiative pathways  $\tau = (k_{\text{rad}} + k_{\text{nonrad}})^{-1}$ , where  $k_{\text{rad}}$  and  $k_{\text{nonrad}}$  are the radiative and nonradiative rates, respectively. Thus, we should be cautious when comparing the experimental lifetime data  $\tau$  to the calculated radiative lifetimes,  $\tau_{\text{rad}} = 1/k_{\text{rad}}$ . However, it has been shown that the reduced PL quantum yield observed in F8BT and F8 systems under pressure is due primarily to the reduced radiative decay rate of the excitons, while the nonradiative decay channels seem to be less affected.<sup>18</sup> The radiative lifetimes  $\tau_{\text{rad}}$  thus serve as an important indicator for the trend of the overall lifetimes  $\tau$ . Calculated radiative lifetimes for geometries resulting in exciplexes reduce with increasing planarization [middle panel of Fig. 3(c)]. However, their behavior as a function of interchain distance is more complex, and two patterns are identified. For the larger torsion angles of 35° and 30° (case 1), the radiative lifetimes decline with reducing interchain distance. However, for the smaller torsion angles of 27° and 25° (case 2), we observe an initial increase followed by a reduction of radiative lifetimes upon decreasing interchain distance. A similar trend as for case 2 is predicted for TFB:F8BT exciplexes [Fig. 4(b)] and is consistent with the pressure-dependent lifetimes measured for TFB:F8BT blends [Fig. 4(a)].

The two behavior patterns can be rationalized by analysis of Eq. (3). Spatial overlap between the wavefunctions increases upon decreasing the interchain distance, which results in stronger electronic couplings  $\langle H_{\text{PFB}} | h | H_{\text{F8BT}} \rangle$  in Eq. (3). This in turn yields an enhanced contribution from the localized excitonic excitation into the lowest CT state. On the other hand, reducing the intermolecular distance may increase  $\Delta E$  because the CT diabatic state is shifted down in energy by the coulomb energy between the bound charges. According to Eq. (3), the increase in  $\Delta E$  acts in the opposite direction compared to the increased electronic coupling and tends to reduce the covalent-ionic mixing. In case 1, the decreasing

radiative lifetimes imply that the overall evolution is driven by the energy mismatch  $\Delta E$ . In case 2, the calculated radiative lifetimes first increase considerably when the interchain distance is compressed. In this range of torsion angles, the CT character thus mostly scales with  $\Delta E$ : reduced D-A spacing implies larger  $\Delta E$ , more prominent CT character, and longer radiative lifetimes. This is because  $\Delta E$  is smaller for less twisted conformers, so a slight change in intermolecular separation strongly perturbs the system and results in large changes in the mixing coefficients. When the interchain distance is decreased further to a critical point (0.03 nm, in this case), the CT diabatic state is strongly stabilized so that  $\Delta E$  takes a substantial value; in this regime, the electronic matrix element is large enough to counterbalance or even exceed the  $\Delta E$  effect. Thus, reduced intermolecular separation translates into larger couplings, increases mixing in the lowest excited state (i.e., reduced CT character), and results in a shortening radiative lifetime.

The lowest panel of Fig. 3(c) shows radiative lifetimes calculated in PFB:F8BT configurations where excitons are the lowest electronic excitations. It is striking to see that the exciton radiative lifetimes are drastically increased when the interchain distance is reduced. This increase (up to a few hundred nanoseconds) indicates admixture of CT character into the covalent states, which is also supported by the excited-state charge distribution. Our finding suggests that by compressing interchain distance by only 0.03 nm, intrachain bulk excitonic excited states may convert into dominant interchain CT excited states. We consider that this is due to an adjustment of the surrounding environment, in which electronic intermolecular interactions and dielectric polarization per unit volume strengthen at a reducing interchain distance. We recall that in the ground-state geometries supporting excitons as the lowest excited states, F8 units of PFB are on top of BT units of F8BT, which locally resembles F8BT-only copolymers. A significantly increased CT character is thus anticipated and has indeed been observed in a pure F8BT film under pressure.<sup>18</sup> Planarization of ground-state geometries also contributes to an increased interchain CT character, yet to a smaller extent than interchain separation.

The calculated polarization of the transition dipole moment with respect to the chain axis, which can be expressed through the angle  $\varphi$ , is consistent with our findings in the radiative lifetimes. The ground-state geometries that lead to excitonic excitations have transition dipole moments primarily polarized along the chain axis. In contrast, the transition dipole moments

## Exciplexes

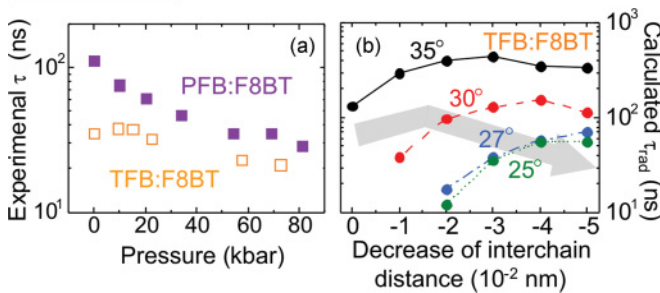


FIG. 4. (Color online) (a) Experimentally observed lifetimes of the exciplexes in PFB:F8BT- and TFB:F8BT-blended thin films as a function of pressure. The lifetimes are determined by fitting the PL decay of the intensity  $I(t)$  at 50–80 and 35–80 ns after excitation for PFB:F8BT and TFB:F8BT blends, respectively, at the energy of the exciplex by the geometric function  $I(t) = I(0)/(1 + t/\tau_x)^\beta$ , where  $\beta = 2.75$ . (b) Calculated excited-state radiative lifetimes of representative TFB:F8BT exciplexes geometries as a function of interchain distance and torsion angle. The gray arrow indicates the trend of the calculated  $\tau_{\text{rad}}$  with increasing pressure, which decreases the intermolecular distance and planarizes the molecular backbone.

TABLE I. INDO/SCI rotational angles  $\varphi$  between the transition dipole moment and the chain axis direction calculated for the lowest excited states of representative (a) exciplex and (b) excitonic geometries in PFB:F8BT blends as a function of the decreased interchain distance ( $\Delta d$ ) and the torsion angle ( $\theta$ ).

	$\theta$	$\Delta d$ (–0.00 nm)	$\Delta d$ (–0.04 nm)
(a) Exciplexes	35°	24.5°	36.4°
	25°	0.6°	23.2°
(b) Excitons	35°	0.4°	3.7°
	25°	0.6°	15.0°

of the ground-state geometries that give rise to CT excitations have a substantial contribution from the stacking direction. Table I shows that for exciplex excitations,  $\varphi$  increases with decreasing interchain distance but decreases with planarization. On the other hand, for ground-state geometries that lead to excitonic excitations, decreasing the interchain distance or planarizing the backbone may significantly enhance the polarizations along the stacking axis.

#### IV. CONCLUSIONS

We have modeled the electronic structure in the lowest excited states of model systems for polyfluorene-based D-A blends and have disentangled the different intramolecular and intermolecular contributions to the pressure-induced PL spectra shifts and changes in lifetimes. These contributions stem from decreased intermolecular distances, increased planarization of the polymers chains, and (to a smaller extent) increased density and dielectric screening. The results of our quantum-chemical calculations are consistent with PL experimental data and point to the following effects:

(1) Redshift of interchain CT-like (ionic) excitations observed under pressure is primarily ascribed to the reduction of the interchain distance, whereas that of intrachain excitonic (covalent) excitations is due to a combined effect of interchain compressibility and planarization. The loss of the structure in the PL spectra is attributed to an increase of vibronic coupling under pressure, which contributes as well to the observed PL shift.

(2) Enhanced exciplex emission may be expected at high pressure because the reducing interchain separation tends to

attenuate the CT character of the polaron pairs and magnify that of the excitons.

(3) The intramolecular excitons may transform into intermolecular CT states under high pressure.

Our work illuminates the important interplay between local geometric configuration, chain conformation, and dielectric environment in shaping the nature of the electronic excited states at D-A polymer interfaces. The use of hydrostatic pressure appears as an elegant way to tune the relative contributions from intermolecular and intramolecular interactions and reveals the rich photophysics of conjugated polymers heterojunctions, which should be useful in designing materials for light-emitting and photovoltaic applications.

#### ACKNOWLEDGMENTS

This work is supported by Engineering and Physical Sciences Research Council, Initial Training Network Supramolecular Functional Nanoscale Architectures for Organic Electronics: A Multi-Site Initial Training Action Grant No. PITN-GA-2009-238177, the NanoSciEra Semiconducting supramolecular nanoscale wires and field-effect transistors, and Comunidad Madrid Grant No. S2009/MAT-1726. The work in Mons, Belgium, was supported by the Interuniversity Attraction Pole program of the Belgian Federal Science Policy Office (PAI 6/27) and Fonds National de la Recherche Scientifique-Fonds de la Recherche Fondamentale Collective. The work in Madrid was supported by a Ramón y Cajal fellowship of the Spanish Ministry for Science and Innovation.

\*ysh21@cam.ac.uk

<sup>1</sup>H. Hoppe and N. S. Sariciftci, *J. Mater. Res.* **19**, 1924 (2004).

<sup>2</sup>R. H. Friend, R. W. Gymer, A. B. Holmes, J. H. Burroughes, R. N. Marks, C. Taliani, D. D. C. Bradley, D. A. D. Santos, J.-L. Brédas, M. Lögdlund, and W. R. Salaneck, *Nature* **397**, 121 (1999).

<sup>3</sup>S. R. Forrest, *Org. Electron.* **4**, 45 (2003).

<sup>4</sup>H. Sirringhaus, *Adv. Mater.* **17**, 2411 (2005).

<sup>5</sup>J. W. Blatchford, S. W. Jessen, L. B. Lin, J. J. Lih, T. L. Gustafson, A. J. Epstein, D. K. Fu, M. J. Marsella, T. M. Swager, A. G. MacDiarmid, S. Yamaguchi, and H. Hamaguchi, *Phys. Rev. Lett.* **76**, 1513 (1996).

<sup>6</sup>W. Graupner, G. Leising, G. Lanzani, M. Nisoli, S. D. Silvestri, and U. Scherf, *Chem. Phys. Lett.* **246**, 95 (1995).

<sup>7</sup>M. Yan, L. J. Rothberg, E. W. Kwock, and T. M. Miller, *Phys. Rev. Lett.* **75**, 1992 (1995).

<sup>8</sup>B. J. Schwartz, *Annu. Rev. Phys. Chem.* **54**, 141 (2003).

<sup>9</sup>J.-L. Brédas, D. Beljonne, V. Coropceanu, and J. Cornil, *Chem. Rev.* **104**, 4971 (2004).

<sup>10</sup>V. Coropceanu, J. Cornil, D. A. d. S. Filho, Y. Olivier, R. Silbey, and J.-L. Brédas, *Chem. Rev.* **107**, 926 (2007).

<sup>11</sup>Y.-S. Huang, S. Westenhoff, I. Avilov, P. Sreearunthai, J. M. Hodgkiss, C. Deleener, R. H. Friend, and D. Beljonne, *Nat. Mater.* **7**, 483 (2008).

<sup>12</sup>M. Chandrasekhar, S. Guha, and W. Graupner, *Adv. Mater.* **13**, 613 (2001).

<sup>13</sup>D. Moses, A. Feldblum, E. Ehrenfreund, A. J. Heeger, T.-C. Chung, and A. G. MacDiarmid, *Phys. Rev. B* **26**, 3361 (1982).

<sup>14</sup>B. C. Hess, G. S. Kanner, Z. V. Vardeny, and G. L. Baker, *Phys. Rev. Lett.* **66**, 2364 (1991).

<sup>15</sup>S.-C. Yang, W. Graupner, S. Guha, P. Puschnig, C. Martin, H. R. Chandrasekhar, M. Chandrasekhar, G. Leising, C. Ambrosch-Draxl, and U. Scherf, *Phys. Rev. Lett.* **85**, 2388 (2000).

<sup>16</sup>J. P. Schmidtke, J.-S. Kim, J. Gierschner, C. Silva, and R. H. Friend, *Phys. Rev. Lett.* **99**, 167401 (2007).

<sup>17</sup>J. P. Schmidtke, R. H. Friend, and C. Silva, *Phys. Rev. Lett.* **100**, 157401 (2008).

<sup>18</sup>S. Albert-Seifried, J. M. Hodgkiss, F. Laquai, H. A. Bronstein, C. K. Williams, and R. H. Friend, *Phys. Rev. Lett.* **105**, 195501 (2010).

<sup>19</sup>V. Morandi, M. Galli, F. Marabelli, and D. Comoretto, *J. Appl. Phys.* **107**, 073106 (2010).

<sup>20</sup>K. Hummer, P. Puschnig, and C. Ambrosch-Draxl, *Phys. Rev. B* **67**, 184105 (2003).

<sup>21</sup>D. Beljonne, Z. Shuai, R. H. Friend, and J.-L. Brédas, *J. Chem. Phys.* **102**, 2042 (1995).

<sup>22</sup>J. Cornil, D. A. d. Santos, X. Crispin, R. Silbey, and J.-L. Brédas, *J. Am. Chem. Soc.* **120**, 1289 (1998).

<sup>23</sup>J. Gierschner, Y.-S. Huang, B. V. Averbeke, J. Cornil, R. H. Friend, and D. Beljonne, *J. Chem. Phys.* **130**, 044105 (2009).

- <sup>24</sup>J. Gierschner, M. Ehni, H.-J. Egelhaaf, B. M. Medina, D. Beljonne, H. Benmansour, and G. C. Bazan, *J. Chem. Phys.* **123**, 144914 (2005).
- <sup>25</sup>J. Gierschner, H.-G. Mack, D. Oelkrug, I. Waldner, and H. Rau, *J. Phys. Chem. A* **108**, 257 (2004).
- <sup>26</sup>C. Lee, W. Yang, and R. G. Parr, *Phys. Rev. B* **37**, 785 (1988).
- <sup>27</sup>A. D. Becke, *J. Chem. Phys.* **98**, 5648 (1993).
- <sup>28</sup>J. Cornil, I. Gueli, A. Dkhissi, J. C. Sancho-Garcia, E. Hennebicq, J.-P. Calbert, V. Lemaire, D. Beljonne, and J.-L. Brédas, *J. Chem. Phys.* **118**, 6615 (2003).
- <sup>29</sup>Accelrys Inc., Molecular Simulations (1996).
- <sup>30</sup>J. Ridley and M. C. Zerner, *Theoret. Chim. Acta* **32**, 111 (1973).
- <sup>31</sup>N. Mataga and K. Nishimoto, *Z. Phys. Chem. Neue Folge* **13**, 140 (1957).
- <sup>32</sup>M. Chandross and S. Mazumdar, *Phys. Rev. B* **55**, 1497 (1997).
- <sup>33</sup>N. S. Bayliss, *J. Chem. Phys.* **18**, 292 (1950).
- <sup>34</sup>X. Cao, B. C. Hancock, N. Leyva, J. Becker, W. Yu, and V. M. Masterson, *Int. J. Pharm.* **368**, 16 (2009).
- <sup>35</sup>S. Westenhoff, I. A. Howard, J. M. Hodgkiss, K. R. Kirov, H. A. Bronstein, C. K. Williams, N. C. Greenham, and R. H. Friend, *J. Am. Chem. Soc.* **130**, 13653 (2008).
- <sup>36</sup>J. Mårdalen, E. J. Samuelsen, O. R. Konestabo, M. Hanfland, and M. Lorenzen, *J. Phys.: Condens. Matter* **10**, 7145 (1998).
- <sup>37</sup>J. Gierschner, H.-G. Mack, H.-J. Egelhaaf, S. Schweizer, B. Doser, and D. Oelkrug, *Synth. Met.* **138**, 311 (2003).
- <sup>38</sup>Experimentally measured PL decays of the exciplex emission are indeed multiexponential, suggesting some heterogeneity in the sample. Usually, we take the delayed emission, e.g., from 50 to 80 ns after excitation, as the exciplex lifetimes.